30. Unimolecular Fragmentation of Energy Selected Allene Molecular Cations

by **Josef Dannacher** and **Jürgen Vogt**

Physikalisch-Chemisches Institut der Universität Basel,
Klingelbergstrasse 80, CH-4056 Basel, Switzerland

(11.XI.77)

Summary

The unimolecular fragmentations of internal energy selected allene molecular ions ($\mathbf{1}^+$) have been investigated by photoelectron-photoion coincidence spectroscopy. The energy dependence of the branching ratio between the two most important fragmentation channels is reported, together with values for the kinetic energy release during fragmentation. Loss of an hydrogen atom from $\mathbf{1}^+$ is interpreted to proceed *via* two paths, yielding different isomeric forms of $C_3H_3^+$ with different kinetic energy release values.

Introduction. - Unimolecular dissociations of excited ions in the gas phase are readily investigated in a mass spectrometer. However, using conventional electron impact or photoionization methods very little is known about the internal energy of the generated ions. On the other hand photoelectron-photoion coincidence spectroscopy yields information concerning the internal energy E_j^* of ions and their fragmentation paths. The results of such coincidence measurements are also needed to test statistical theories of unimolecular reactions applied to ions [1] [2].

The ions are generated by photoionization with 58.4 nm (He(Iα)) photons. Using radiation of fixed energy has the advantage that the experiments are not affected by autoionization and threshold law assumptions. Thus the ionization energy I_j of the parent molecule is defined as the difference between the energy hν of the ionizing radiation and the kinetic energy of the photoelectron $T(e^-)$.

$$I_j = h\nu - T(e^-) \tag{1}$$

The internal energy E_j^* of the resulting molecular ion is defined as

$$E_j^* = I_j - I_1^a, \tag{2}$$

where I_1^a is the first adiabatic ionization energy of the parent molecule, *i.e.* the energy of the transition to the radical cation in its doublet ground state. The excess energy can be lost by fluorescence or, alternatively, by fragmentation which can occur with or without a preceding internal conversion and/or an isomerization proceeding with $E_j^* = \text{const.}$ By detecting a mass selected ion in coincidence with its corresponding photoelectron of known energy $T(e^-)$ coincidence spectra are obtained.

In the present work we report the coincidence spectra of allene (**1**). The monomolecular fragmentation of excited allene cation ($\mathbf{1}^+$) is of interest, in particular with

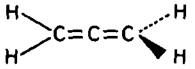

1

$$H{-}C{\equiv}C{-}CH_3$$

2

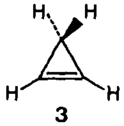

3

$$H{-}C{\equiv}C{-}CH_2^{\oplus}$$

4$^{\oplus}$

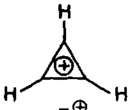

5$^{\oplus}$

respect to the fragmentation of propyne cation ($\mathbf{2}^+$) and cyclopropene cation ($\mathbf{3}^+$), both of which are isomers of $\mathbf{1}^+$. The energy dependence of the branching ratio for the following two reactions and the kinetic energy released during fragmentation

$$C_3H_4^+ \longrightarrow C_3H_3^+ + H \tag{1}$$

$$C_3H_4^+ \longrightarrow C_3H_2^+ + H_2 \tag{2}$$

have been measured. The extent to which the isomeric $C_3H_3^+$ ions, propargyl cation ($\mathbf{4}^+$) and cyclopropenyl cation ($\mathbf{5}^+$) are formed, is discussed.

Experimental procedure. - The photoelectron-photoion coincidence spectrometer used is schematically shown in *Figure 1*. In the photoionization source a beam of He(Iα) radiation is crossed with a sample gas jet. Photoelectrons and photoions are collected in opposite directions by applying a suitable electrostatic field. The photoelectrons are energy selected using a $\pi/\sqrt{2}$ cylindrical electrostatic analyser. The ions are accelerated and focused into a quadrupole mass spectrometer. Photoelectron spectra and photoion mass spectra are obtained by counting electrons and ions individually.

In order to detect in coincidence an ion (k) of mass m_k and its corresponding electron the difference in the time of flight of the electron and the ion has to be taken into account. Therefore the electron signal is delayed by an appropriate delay-time t_d depending on the mass m_k and then converted into a pulse of defined width τ which constitutes the acceptance time of the coincidence gate.

In the first type of coincidence experiments a particular ion mass m_k is selected. The delay time t_d is set to match the ion flight time and the optimum coincidence gate width τ is chosen. Then by scanning $T(e^-)$ *i.e.* the ionization energy I_j the branching ratio $b = b\ (I_j, m_k)$ is obtained. The latter is the fraction of ions of mass m_k originating from molecular ions produced with an internal energy E_j^* corresponding to I_j. Time-of-flight distributions (TOF-distributions) for ions of

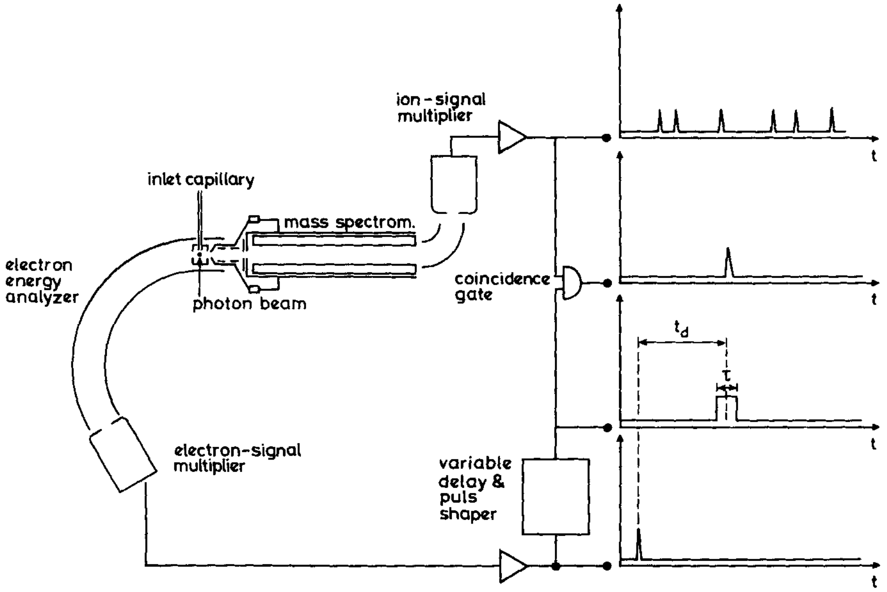

Fig. 1. *Scheme of the photoelectron-photoion coincidence spectrometer and of the coincidence electronics*

mass m_k can be measured by a second type of coincidence experiment. For a fixed ionization energy I_j only ions of predetermined mass m_k are allowed to pass through the mass filter. A very small gate width τ is chosen and the delay time t_d is scanned.

Evaluation of Coincidence Data. - Due to inevitable non-ideal features of the photoelectron-photoion coincidence spectrometer the directly measured coincidence data have to be corrected in an appropriate manner. The statistics of the coincidence experiment has been discussed by *Eland* [3]. The procedures given there have been adapted, allowing for the specific facilities of our spectrometer, *e.g.* the simultaneous mass filtering of the ions and the kinetic energy analysis of the photoelectrons [4].

The coincidence rate $C=C\,(I_j, m_k)$ for a molecular or fragment ion of mass m_k, originating from the molecular ion of energy I_j and its corresponding photoelectron is given ideally by equation (3), with f_i and f_e representing the transmission coefficients of the mass filter and the photoelectron spectrometer, respectively:

$$C = f_e f_i \, b\,(I_j, m_k)\, N\,(I_j)\, \Phi \qquad (3)$$

As mentioned above $b\,(I_j, m_k)$ denotes the branching ratio and $N\,(I_j)$ is the formation rate of molecular ions of ionization energy I_j. The function Φ accounts for the TOF-distribution of the ions due to their individual kinetic energies (see below).

In principle, C could be measured directly, if the delay time t_d, correcting for the different flight times of ions and electrons was sharply defined, and if the coincidence gate width τ could be chosen infinitely narrow. Instead, with finite τ, random coincidences of rate C_r are always measured independently of the delay time t_d. Consequently, even with the correct t_d, only the sum of random (C_r) and true (C_t) coincidences with rate C_{tot} is measurable:

$$C_{tot} = C_t + C_r \tag{4}$$

For convenience, we introduce the following definitions.

a) $N_e(I_j)$ denotes the count rate of photoelectrons with a kinetic energy $T = h\nu - I_j$, as given in (1):

$$N_e(I_j) = f_e N(I_j) \tag{5}$$

b) $N_i(m_k)$ is the count rate of ions of given mass m_k, which stem from the molecular ions produced in the ion source in various states:

$$N_i(m_k) = f_i \sum_{I_j} [b(I_j, m_k) N(I_j)] \tag{6}$$

c) The rate of true coincidences $C_t = C_{tot} - C_r$ (*cf.* (4)) has to be corrected for the paralysis in the coincidence gate and for the background electron count rate $N_{e,noise}$ to yield the coincidence rate (3):

$$C(I_j, m_k) = C_t \left(\frac{1}{1-P}\right) \left(\frac{N_e(I_j)}{N_e(I_j) - N_{e,noise}}\right) \tag{7}$$

In this equation, the factor $1/(1-P)$ accounts for the paralysis in the coincidence gate, with P given as

$$P = \frac{N_i(m_k)\tau}{1 + N_i(m_k)\tau}. \tag{8}$$

With an ion count rate $N_i(m_k) \approx 10^5\ s^{-1}$, an ion background count rate of a few counts per second can be neglected.

The count rates of ions, $N_i(m_k)$, of electrons, $N_e(I_j)$, and of coincidences, C_{tot} and C_r, can be measured independently. With these data and using equations (3) and (7), the branching ratios $b(I_j, m_k)$ are obtained under the assumption of constant spectrometer transmission coefficients f_e and f_i. In principle, these coefficients are dependent on energy and mass of the particles to be analysed, but they are taken to be constant in this study.

For ions which are only formed with thermal kinetic energy, a gaussian TOF-distribution will result [5] [6]. *Figure 2a* shows the TOF-distribution for argon ions fitted to a gaussian distribution by a least squares difference procedure [7]. The ions have been generated from thermal argon gas of 300 K, corresponding to 40 meV kinetic energy of the argon atoms and thus of the ions. The full width at half maximum w is a function of this average kinetic energy.

The effect of using a capillary as inlet for the sample gas is evident from *Figure 2b*. The TOF-distribution of the ions is considerably less broadened due to the directional effect of the capillary on the thermal motion of the argon atoms and to the cooling effect by expansion into vacuum. The lower average kinetic energy

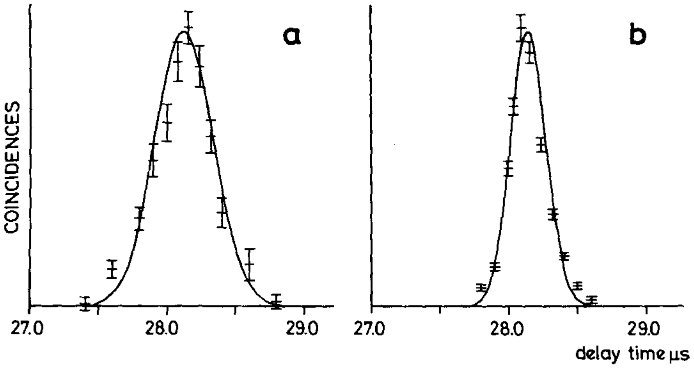

Fig. 2. *Time-of-flight distributions of argon ions*
a) without capillary inlet system; b) with use of a 0.35 mm i.d. steel capillary as inlet

perpendicular to the axis of the gas jet corresponds to an apparent temperature of about 110 K. This sharp reduction of the width of the TOF-distribution is essential for quantifying small values of kinetic energy released during fragmentation.

Fragment ions can be formed with excess kinetic energy depending on the mechanism and the energetics of the fragmentation and the internal energy E_j^* of the parent ion. The extra kinetic energy will broaden the TOF-distribution for that ion. Magnitude and distribution of the kinetic energy released during fragmentation can be deduced from the experimental TOF-distribution measured with a good signal to noise ratio, as was demonstrated by several authors [8] [9]. Assuming that the released kinetic energy has a maxwellian distribution, as was shown to be approximately true for some cases [9], again a gaussian TOF-distribution of the fragment ions will result [5] [8]. This distribution, however, will have a larger w compared to that of thermal ions. From this broadening an average kinetic energy release can be determined. Results for fragment ions from $\mathbf{1}^+$ are discussed in the following section.

Results and Discussion. - The photoelectron spectrum of **1** and the coincidence spectra for the molecular ion $\mathbf{1}^+$ and the fragment ions $C_3H_3^+$ and $C_3H_2^+$ are shown in *Figure 3.* Coincidences for the molecular ion are detected only with electrons associated with the first band ① in the photoelectron spectrum. This means that the ionization energy $I_1 \approx 10$ to 11 eV lies below fragmentation threshold, in agreement with the measured fragment appearance potentials [10] [11] [12]. No coincidences with molecular ions are observed for electrons corresponding to the higher energy photoelectron bands ② and ③, which leads to the conclusion that (i) fragmentations are fast on the microsecond time scale of the spectrometer and (ii) that excited ions do not fluoresce. The latter conclusion is supported by ion fluorescence experiments [13] where no emission was observed from excited allene cations. The molecular ions formed in states corresponding to the 14 to 18 eV photoelectron-bands ② and ③ dissociate to yield $C_3H_3^+$ and $C_3H_2^+$ fragment ions (reactions (1) and (2)).

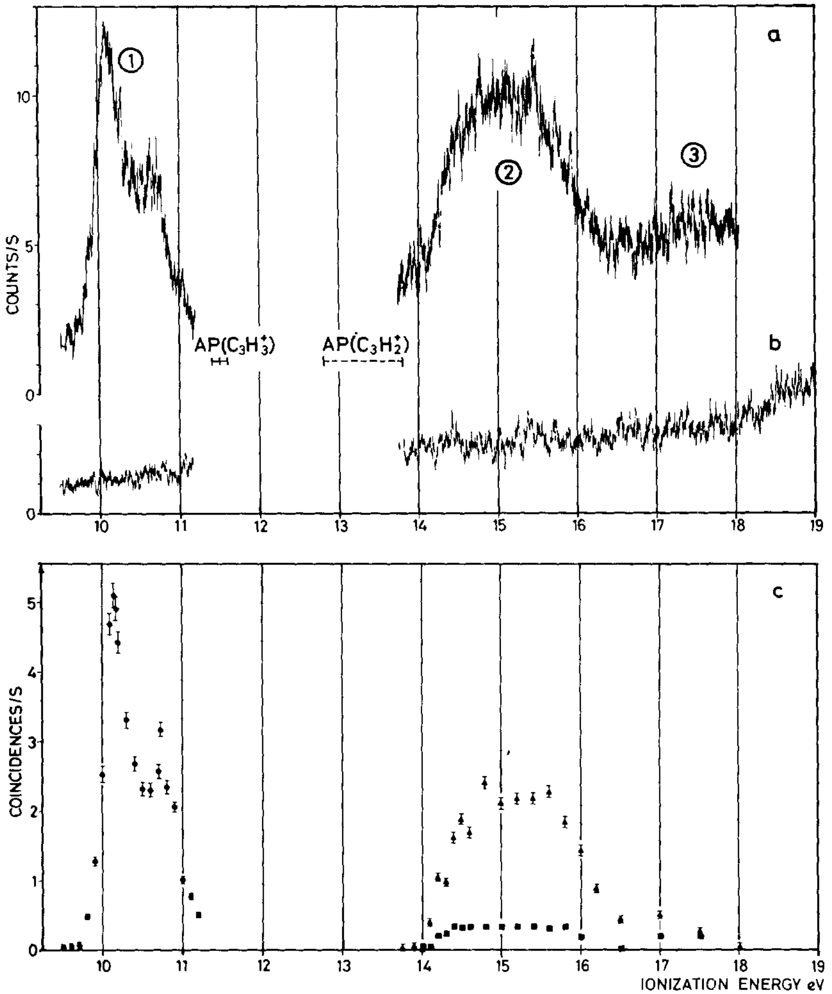

Fig. 3. *Coincidence spectra of allene* (**1**)

a) photoelectron spectrum under coincidence conditions; b) background electrons; c) coincidence spectra for 1^+ (*m/e* 40, ●), $C_3H_3^+$ (*m/e* 39, ▲) and $C_3H_2^+$ (*m/e* 38, ■)

The appearance potential (AP.) for the formation of $C_3H_3^+$ generated from **1** is well established to be 11.48 eV [10] [11]. From this and data obtained from other precursors it is concluded, that $C_3H_3^+$ is formed as cyclopropenyl cation $\mathbf{5}^+$ at threshold [11] [14]. The ionization potential of propargyl radical **4** being 8.68 eV [11], the fragment $\mathbf{4}^+$ is estimated to be about 105 kJ mol^{-1} less stable than $\mathbf{5}^+$. Thus the calculated AP. of $\mathbf{4}^+$ generated from **1** is ≈ 12.5 eV. Consequently from molecular ions $\mathbf{1}^+$ formed with an energy corresponding to the onset of band ②, *i.e.* $I_j > \approx 14$ eV, both isomeric $C_3H_3^+$ ions can be reached. The AP. of $C_3H_2^+$, determined by electron impact, has been quoted as 14.34 eV [12], a value somewhat more uncertain than the one quoted for $C_3H_3^+$. Our experiments have shown that $C_3H_2^+$

ions are already formed at 14.1 ± 0.1 eV. The amount of kinetic energy released during fragmentation (2) *(Table 1)* suggests that the AP. should be even lower than 14 eV. With 1527 kJ mol^{-1} as heat of formation of $C_3H_2^+$ *(Table 2)*, an AP. of 13.8 eV from **1** is calculated.

The branching ratio between reactions (1) and (2) is found to be about 6:1 and fairly constant over the ionization energy range from 14.0 to 16.5 eV. Because several electronically excited states of the parent cation **1**$^+$ lie in this range [15], the absence of sudden changes in the branching ratio indicates that there is no isolated state dissociation [16]. We observe for the photoelectron band ③ (16.7 to 18 eV) a branching ratio of about 3:2 for reactions (1) and (2). Possibly there is some formation of C_3H^+ ions from cations **1**$^+$ belonging to this energy range; however, we did not attempt to observe coincidences because of the low count rate

Table 1. *Mean kinetic energies* a) *released during fragmentation of* **1**$^+$

Fragment ion	Internal energy b) of parent ion	Kinetic energy c) d) on fragment ion	Total kinetic energy release d) e)
$C_3H_3^+$	5.1	43	1.7
$C_3H_3^+$	5.9	24	0.96
$C_3H_2^+$	5.1	79	1.6
$C_3H_2^+$	5.9	44	0.88

a) Determined from the gaussian distributions fitted to the experimental TOF-distributions *(Figure 4)*.
b) In eV, ± 0.1 eV.
c) In meV.
d) ± 25% as given by the standard deviations of the fitted gaussian distributions.
e) In eV.

Table 2. *Thermodynamic values*

Neutral	ΔH_f° 298(g) a)	I_1 a) b)	ΔH_f° 298(g) (cation) a)
1	192 c)	9.68 d) 9.70 e)	1125
2	185 c)	10.36 f)	1185
3	276 c)	9.70 e)	1212
4			1176 g)
5			1080 g) h)
C_3H_2			1527 i) j)

a) In kJ mol^{-1}.
b) Adiabatic ionization potential, in eV.
c) *H.M. Rosenstock, K. Draxl, B.W. Steiner & J.T. Herron*, J. phys. Chemistry Ref. Data *6*, Suppl. 1 (1977).
d) *R.K. Thomas & H. Thompson*, Proc. Roy. Soc. *A 339*, 29 (1974).
e) *P. Bischof & E. Heilbronner*, Helv. *53*, 1677 (1970).
f) *P. Carlier, J.E. Dubois, P. Masclet & G. Mouvier*, J. Electron Spectrosc. *7*, 55 (1975).
g) See [11].
h) See [10].
i) *J.L. Franklin, J.G. Dillard, H.M. Rosenstock, J.T. Herron, K. Draxl & F.H. Field*, Natl. Bureau of Standards U.S., Stand. Ref. Data Ser. *26* (1969).
j) Taken only as upper limit (see text).

of C_3H^+. *Figure 4* shows the TOF-distributions of parent and fragment ions of **1**. The broadening of the distributions for the fragment ions due to kinetic energy release during fragmentation is apparent. The values for the mean kinetic energy

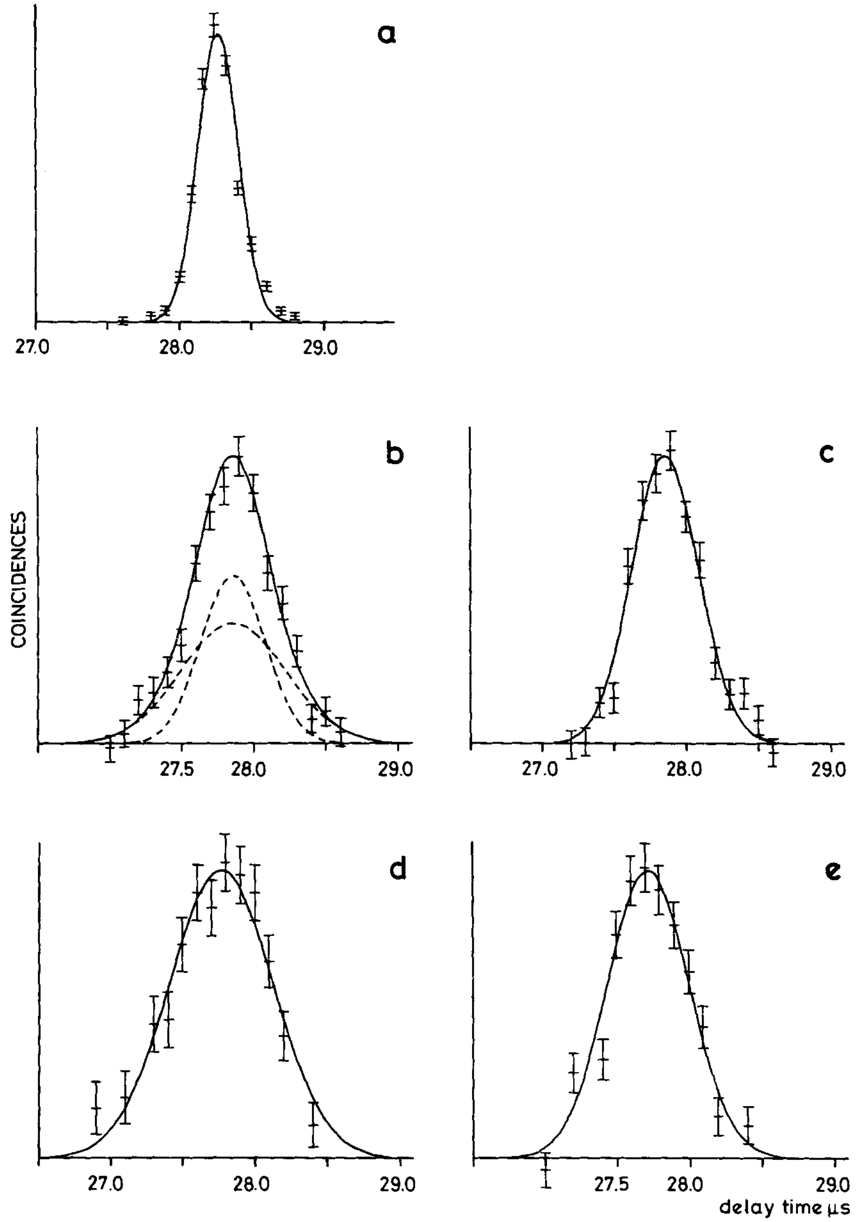

Fig. 4. *Time-of-flight (TOF) distributions of molecular and fragment ions of allene*
a) molecular ion 1^+; b), c) fragment ion $C_3H_3^+$ at internal energies of 5.1 eV and 5.9 eV, respectively
d), e) fragment ion $C_3H_2^+$ at internal energies of 5.1 eV and 5.9 eV, respectively

release determined from the TOF-distributions are listed in *Table 1*. These values are not very accurate due to the unfavourable mass ratio of neutral to charged fragments. Nevertheless, the results demonstrate that it is possible to measure kinetic energy releases even for loss of 1 or 2 H from excited ions with our coincidence spectrometer. From the shape of the metastable ion signal observed in a conventional mass spectrometer, *Holmes & Terlouw* [18] concluded that the mean kinetic energy release for reaction (1) is 170 meV. A comparison with our value of ≥ 960 meV *(Table 1)* indicates that those metastable ions are formed with far less internal energy.

It is an intriguing question whether the formation of the two isomeric $C_3H_3^+$ ions, $\mathbf{4}^+$ and $\mathbf{5}^+$, is accompanied by the release of different amounts of kinetic energy. This phenomenon was already observed by *Baer et al.* [17] for $C_3H_3^+$ fragment ions from propargyl halides, where the higher energy isomer $\mathbf{4}^+$ is formed with less kinetic energy than $\mathbf{5}^+$. The yield of the latter decreases with increasing internal energy of the parent ion [17]. Lead by these experimental findings we tentatively interpreted the TOF-distributions of $C_3H_3^+$ as a sum of two gaussian distributions with different half-widths. The results of a least squares fitting procedure negated the presence of two components in the TOF-distribution of $C_3H_3^+$ at an internal energy E^* of 5.9 eV *(Figure 4c)* but indicated that the TOF-distribution for the ions, with $E^* = 5.1$ eV *(Figure 4b)* can be deconvoluted into two gaussian distributions corresponding to kinetic energy releases of 0.9 eV and 3.1 eV. Although this deconvolution is hardly significant it does not exclude the presence of two kinetic energy release components. We hope to get further insight by recording TOF-distributions with better signal to noise ratio in the near future.

It is rather surprising that reactions (1) and (2) lead to a fairly constant fragment ratio over a wide energy range independent of the internal energy E^* of $\mathbf{1}^+$, especially in view of the large difference in experimental threshold energies. Similar competition has been observed only with secondary fragmentations where a primary process leads to ions having a broad distribution of internal energies [19]. A possible explanation for this effective competition can be rationalized in terms of the isomerization mentioned above. In the subsequent discussion we consider possible isomerization reactions of $\mathbf{1}^+$ into $\mathbf{2}^+$ and/or $\mathbf{3}^+$ competing with the direct fragmentations (1) and (2). The isomerized parent ions could fragment *via* different reaction channels with individual activation energies and rate constants.

From the symmetrical TOF distributions of the fragment ions *(Figure 4)* we conclude that the overall rates of the fragmentation processes are fast compared to the time scale of our experiment. Rate constants of the order of 10^6 s^{-1} or smaller would asymmetrically broaden the TOF-distributions due to fragmentations during ion acceleration [20].

To rationalize the observed branching ratio, rate constants for the fragmentation pathways were calculated using the quasi-equilibrium theory (QET.). Including isomerization leading from one of the excited ions $\mathbf{1}^+$, $\mathbf{2}^+$ or $\mathbf{3}^+$ to another (and which are likely to occur below or at the lowest fragmentation threshold [10] [11]) the reactions (3) to (8) have to be taken into consideration as possible fragmentation paths for the $C_3H_4^+$ parent cations.

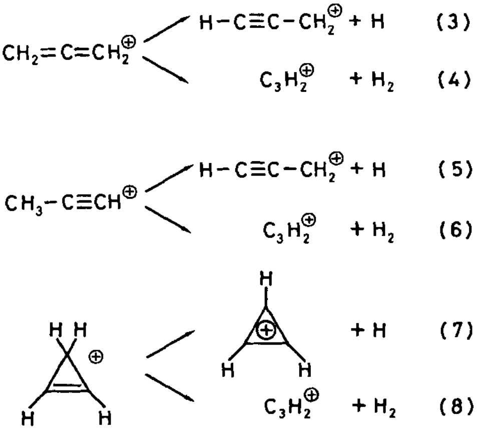

For these reactions monomolecular rate constants have been obtained from QET.-calculations within the approximation described by *Vestal et al.* [21] using a computer program written by *Buttrill* [22]. Normal mode frequencies for the molecular ions and the transition state complexes have been chosen according to [23]. The choice of these frequencies is not critical, because the calculated rate constants are not very sensitive to changes in the frequencies [23]. Furthermore, we use only the relative magnitudes of the rate constants for a qualitative discussion of the branching ratio.

The activation energies for the hydrogen atom abstractions were calculated using the experimental heats of formation given in *Table 2*, assuming that the ions **1**$^+$ and **2**$^+$ yield **4**$^+$ on fragmentation (reactions (3) and (5)), and that only **3**$^+$ yields **5**$^+$ (reaction (7)). Thermodynamical data for the H_2 abstraction from the precursors **1**$^+$, **2**$^+$, and **3**$^+$ are less well documented, because the structures of the several possible isomeric $C_3H_2^+$ fragment ions and the corresponding heats of formation are unknown. For our calculations we used the heat of formation of $C_3H_2^+$ mentioned above *(cf. Table 2)*, which is assumed to be independent of the precursor. For the characterization of the activated complex, the elimination of H_2 is postulated to proceed *via* a 1,3-mechanism for reaction (4) and a 1,1-mechanism for reactions (6) and (8). Other possible mechanisms lead probably to higher energy fragment ions and are thus kinetically less favoured. Inclusion of these mechanisms would slightly increase the overall reaction rate for (2) by, at most, a factor of four, which, however, does not affect the arguments given below.

The results of the QET. calculations are given in *Table 3*. For an ionization energy above 14 eV the rate constants for reactions (1) and (2) are calculated to be larger than 10^6 s^{-1} in accordance with the experimentally found symmetric TOF-distributions of the fragment ions. Taking the appearance potential (AP.) of $C_3H_2^+$ as 13.8 eV, the calculations predict reaction (1) to be about two orders of magnitude faster than (2) irrespective of the structure of the parent ion. This means, that practically all excited molecular ions would react according to (1), and thus produce only $C_3H_3^+$ ions. With an assumed AP. of 12.8 eV for $C_3H_2^+$, *i.e.* 1 eV lower than derived above, the QET. model accounts for the experimental results reasonably

Table 3. *Calculated unimolecular dissociation rate constants* a)

Parent ion	Reaction	Internal energy E^* b)		
		4.5	5.1	5.9
	1	1.1 (9)	4.9 (10)	1.9 (11)
1$^+$	2	2.1 (6)	2.2 (8)	6.3 (9)
	2 c)	2.5 (10)	8.3 (10)	4.4 (11)
	1	3.6 (11)	1.5 (12)	5.6 (12)
2$^+$	2	2.4 (7)	1.9 (9)	4.5 (10)
	2 c)	1.3 (11)	6.9 (11)	3.2 (12)
	1	9.0 (12)	1.4 (13)	2.2 (13)
3$^+$	2	9.4 (6)	5.5 (8)	1.1 (10)
	2 c)	3.6 (10)	1.8 (11)	7.2 (11)

a) In s^{-1}, 1.1 (9) to be read as 1.1×10^9.

b) In eV, relative to ground state **1**$^+$.

c) AP($C_3H_2^+$) assumed as 12.8 eV, see text.

well. As can be seen from the rate constants for the latter AP. *(Table 3)*, reaction (2) starting from **1**$^+$ becomes faster than (1). The direct fragmentation of **1**$^+$ into $C_3H_2^+$ in competition with an isomerization to **2**$^+$ or **3**$^+$ and subsequent fast fragmentation yielding $C_3H_3^+$ would qualitatively account for the experimental branching ratio. The overall reaction *i.e.* isomerizations and loss of hydrogen atoms, thus yields both acyclic and cyclic $C_3H_3^+$ ions, which is in agreement with the interpretation of the TOF-distributions given above.

After completion of this work we became aware of a complementary study by *Stockbauer et al.* [24] on allene using the threshold photoion-photoelectron coincidence technique. The only comparable results are the branching ratios which are in good agreement. Values are given for the AP. of $C_3H_2^+$ from **1** measured by photoionization as 13.5±0.2 eV and by the threshold coincidence technique as 13.0±0.1 eV. The latter is very close to the value of 12.8 eV which is used in our QET. calculations.

Experimental Part. - A double stage differentially pumped He-resonance lamp is used as source of He(Iα) radiation (21.22 eV) collimated by a capillary and two circular apertures to a diameter of 0.3 mm. The sample is introduced through a hypodermic needle (0.35 mm) as a gas-jet which intersects the photon beam. The support of the needle is movable in all three dimensions for proper alignment. Ionization takes place in a weak electrostatic field of about 4 V/cm which extracts the charged particles out of the source. The magnitude of the field strength F_s in the source is a crucial parameter of such photoelectron-photoion coincidence experiments. It affects the transmission coefficients, f_e and f_i, of both spectrometers, the resolution of the PE.-energy analyser and the optimum coincidence gate width τ.

The electrons are energy analysed in a conventional 10 cm radius 127°-analyser (*Perkin Elmer* PS 18). Within a small range the desired resolution/transmission ratio can be adjusted by varying the width of the exit slit of the analyser. The electrons are registered as single pulses using a *Venetian Blind* multiplier (EMI 9643).

The ions are focused by a four stage electrostatic lens system into a quadrupole mass spectrometer (*Balzers* QMG 511). The use of such a mass filter yields unity resolution over the whole accessible mass range (1 to 511), whereas the resolution of pure time-of-flight mass analysis is affected by high kinetic energy ions. A broadening of the TOF-distributions due to the quadrupole radio frequency was eliminated by appropriate filtering of all electrostatic potentials.

Two oil diffusion pumps (*Edwards* Diffstak, 200 dm^3 s^{-1}) maintain the necessary high vacuum. A typical background pressure of 10^{-7} Torr is obtained. Under operating conditions the pressure ranges from 10^{-7} to 10^{-6} Torr.

Under coincidence conditions the coincidence spectrometer shows a photoelectron energy resolution of 140 mV full width at half maximum as measured with argon as sample gas. Typical values for f_i and f_e are 0.45 and $2 \cdot 10^{-4}$, respectively, yielding about ten coincidences per second at an ionization rate on the order of 10^5 s^{-1}.

The photoionization mass spectrum of commercially available allene used for our experiments showed only ions at *m/e* 40 (relative intensity, corrected for ^{13}C: 95), 39 (100), 38 (24), and 37 (3). No significant amounts of fragment ions formed *via* C–C bond cleavage were detected. According to the mass spectrum no impurities were present.

This work is part Cl of project No. 2.518-0.76 of the *Schweizerischer Nationalfonds zur Förderung der wissenschaftlichen Forschung*. We thank *S.E. Buttrill jr.* for a listing of the QET. program. Support by *Ciba-Geigy SA, F. Hoffmann-La Roche & Cie SA* and *Sandoz SA* (Basel) is gratefully acknowledged.

REFERENCES

[1] *R.A. Marcus & O.K. Rice*, J. phys. Colloid Chemistry *55*, 894 (1951); *G.M. Wieder & R.A. Marcus*, J. chem. Physics *37*, 1835 (1962).
[2] *H.M. Rosenstock, M.B. Wallenstein, A.L. Wahrhaftig & H. Eyring*, Proc. Nat. Acad. Sci. U.S. *38*, 667 (1952).
[3] *J.H.D. Eland*, Int. J. Mass Spectrom. Ion Physics *8*, 143 (1972); *M.E. Gellender & A.D. Baker*, Int. J. Mass Spectrom. Ion Physics *17*, 1 (1975).
[4] *J. Dannacher*, Ph. D. Thesis, University of Basel 1976.
[5] *J.L. Franklin, P.M. Hierl & D.A. Whan*, J. chem. Physics *47*, 3148 (1967).
[6] *A. Harvey, M.L. Monteiro & R.I. Reed*, Int. J. Mass Spectrom. Ion Physics *4*, 365 (1970).
[7] *U. Hoffmann & H. Hofmann*, Einführung in die Optimierung, Verlag Chemie, Weinheim 1971.
[8] *H.E. Stanton & J.E. Monahan*, J. chem. Physics *41*, 3694 (1964).
[9] *B. Brehm, J.H.D. Eland, R. Frey & A. Küstler*, Int. J. Mass Spectrom. Ion Physics *12*, 197 (1973); *D.M. Mintz & T. Baer*, J. chem. Physics *65*, 2407 (1976).
[10] *A.C. Parr & G.A. Elder*, J. chem. Physics *49*, 2659 (1968); *C.S. Mathews & P. Warneck*, J. chem. Physics *51*, 854 (1969).
[11] *F.P. Lossing*, Canad. J. Chemistry *50*, 3973 (1972).
[12] *J.L. Franklin & A. Mogenis*, J. phys. Chemistry *71*, 2820 (1967).
[13] *J.P. Maier*, private communication.
[14] *A.S. Werner & T. Baer*, J. chem. Physics *62*, 2900 (1975).
[15] *D.W. Turner, C. Baker, A.D. Baker & C.R. Brundle*, 'Molecular Photoelectron Spectroscopy', Wiley-Interscience, New York 1970.
[16] *J.H.D. Eland*, Int. J. Mass Spectrom. Ion Physics *13*, 457 (1974).
[17] *B.P. Tsai, A.S. Werner & T. Baer*, J. chem. Physics *63*, 4384 (1975).
[18] *J.L. Holmes & J.K. Terlouw*, Org. Mass Spectrom. *10*, 787 (1975).
[19] *B. Brehm, J.H.D. Eland, R. Frey & H. Schulte*, Int. J. Mass Spectrom. Ion Physics *21*, 373 (1976).
[20] *T. Baer, B.P. Tsai, D. Smith & P.T. Murray*, J. chem. Physics *64*, 2460 (1976).
[21] *M. Vestal, A.L. Wahrhaftig & W.H. Johnston*, J. chem. Physics *37*, 1276 (1962).
[22] *S.E. Buttrill jr.*, J. chem. Physics *52*, 6174 (1970).
[23] *M.L. Vestal*, in Fundamental Processes in Radiation Chemistry, P. Ausloos (editor), Wiley-Interscience, New York 1968.
[24] *A.C. Parr, A.J. Jason & R. Stockbauer*, private communication to Dr. *J.P. Maier*.